NIH Public Access
Author Manuscript
Aging Cell. Author manuscript; available in PMC 2014 December 01.

Published in final edited form as:
Aging Cell. 2013 December ; 12(6): . doi:10.1111/acel.12127.

Lipoic Acid Restores Age-Associated Impairment of Brain Energy Metabolism through the Modulation of Akt/JNK Signaling and PGC1α Transcriptional Pathway

Tianyi Jiang, **Fei Yin**, **Jia Yao**, **Roberta Díaz Brinton**, and **Enrique Cadenas**[ζ]
Pharmacology & Pharmaceutical Sciences, School of Pharmacy, University of Southern California, Los Angeles, CA 90089, USA

Summary

This study examines the progress of a hypometabolic state inherent in brain aging with an animal model consisting of Fischer 344 rats of young, middle, and old ages. Dynamic microPET scanning demonstrated a significant decline in brain glucose uptake at old ages, which was associated with a decrease in the expression of insulin-sensitive neuronal glucose transporters GLUT3/4 and of microvascular endothelium GLUT1. Brain aging was associated with an imbalance of the PI3K/Akt pathway of insulin signaling and JNK signaling and a downregulation of the PGC1α – mediated transcriptional pathway of mitochondrial biogenesis that impinged on multiple aspects of energy homeostasis. R-(+)-lipoic acid treatment increased glucose uptake, restored the balance of Akt/JNK signaling, and enhanced mitochondrial bioenergetics and the PGC1α-driven mitochondrial biogenesis. It may be surmised that impairment of a mitochondria-cytosol-nucleus communication is underlying the progression of the age-related hypometabolic state in brain; the effects of lipoic acid are not organelle-limited but reside on the functional and effective coordination of this communication that results in improved energy metabolism.

Keywords

Brain aging; Lipoic Acid; Mitochondria; Insulin signaling; JNK signaling; PGC1α; Sirt1; Mitochondrial Biogenesis; Mitochondrial Bioenergetics; FDG-PET; Mitochondrial Metabolism

Introduction

Brain is a highly energy-demanding organ, which represents only 2% of the body weight but accounts for 25% of the total glucose utilization. Brain aging features pronounced energy deficit accompanied by neuronal loss, impaired cognition and memory, and increased risk for neurodegenerative disorders. This hypometabolic state is a consequence of a decreased energy-transducing capacity of mitochondria, partly attributed to reduced rates of electron transfer, decreased inner membrane potential, and impaired ATPase activity (Navarro &

[ζ]*To whom correspondence should be addressed* Enrique Cadenas Pharmacology & Pharmaceutical Sciences School of Pharmacy University of Southern California 1985 Zonal Avenue Los Angeles, CA 90089 cadenas@usc.edu.
TJ: tianyiji@usc.edu
FY: feiyin@usc.edu
JY: jiayao@usc.edu
RDB: rbrinton@usc.edu
EC: cadenas@usc.edu

Author Contributions
The experiments were designed by TJ and EC, and carried out by TJ, FY, and JY with RDB assistance. The manuscript was prepared by TJ and EC.

NIH-PA Author Manuscript
NIH-PA Author Manuscript
NIH-PA Author Manuscript

NIH-PA Author Manuscript

NIH-PA Author Manuscript

NIH-PA Author Manuscript

Boveris 2007). The activity of enzymes or complexes that catalyze the entry of acetyl-CoA into the tricarboxylic acid cycle, *i.e.*, pyruvate dehydrogenase and succinyl-CoA transferase, decreases as a function of age in brain (Lam *et al.* 2009; Zhou *et al.* 2009), as well as the activity of the tricarboxylic acid regulatory enzyme, α-ketoglutarate dehydrogenase (Gibson *et al.* 2004). Mitochondrial biogenesis could be viewed as an adaptive response to adjust bioenergetic deficits to alterations in the extracellular and intracellular energy–redox status (Onyango *et al.* 2010).

Mitochondria are effective sources of H_2O_2, which is involved in the regulation of redox-sensitive signaling and transcriptional pathways. Mitochondrial function is also regulated by signaling and transcriptional pathways (Yin *et al.* 2012; Yin *et al.* 2013). The PI3K/Akt route of insulin signaling is implicated in neuronal survival and synaptic plasticity, via – among other effects– maintenance of the functional integrity of the mitochondrial electron transfer chain and regulation of mitochondrial biogenesis (Cohen *et al.* 2004; Cheng *et al.* 2010); conversely, mitochondrially generated H_2O_2 plays an important role in the insulin receptor (IR) autophosphorylation in neurons (Storozhevykh *et al.* 2007). In human neuroblastoma cells, Akt translocates to the mitochondrion and subunit β of ATPase is a phosphorylation target (Bijur & Jope 2003). Mitochondrial oxidants are also involved in the activation of c-Jun N-terminal kinase (JNK) (Nemoto *et al.* 2000; Zhou *et al.* 2008), which, in turn, regulates mitochondrial bioenergetics by modulating the activity of pyruvate dehydrogenase in primary cortical neurons (Zhou *et al.* 2008). JNK translocates to the mitochondrion and associates with the outer mitochondrial membrane and triggers a phosphorylation cascade that results in phosphorylation (inhibition) of the pyruvate dehydrogenase complex; there is an inverse relationship between the increasing levels of active JNK associated with the outer mitochondrial membrane and the decreasing pyruvate dehydrogenase activity in rat brain as a function of age (Zhou *et al.* 2009). This translated into decreased cellular ATP levels and increased lactate formation.

R-(+)-lipoic acid (1,2-dithiolane-3-pentanoic acid) acts as a cofactor in energy metabolism and the non-covalently bound form as a regulator of the cellular redox status. The effects of lipoic acid on the cellular energy and redox metabolism, physiology, and pharmacokinetics have been extensively reviewed (Patel & Packer 2008; Shay *et al.* 2009). Lipoic acid modulates distinct redox circuits because of its ability to equilibrate between different subcellular compartments as well as extracellularly and is an essential cofactor for the mitochondrial E_2 subunit of α-ketoacid dehydrogenase complexes. As a potent redox modulator, lipoic acid participates in a wide variety of biological actions based mainly on thiol-disulfide exchange reactions with key redox-sensitive cysteines on target molecules. Considering the variety of redox-sensitive signaling and transcriptional pathways regulating brain energy metabolism, lipoic acid has potential of modulating the cellular energy and redox status.

This study was aimed at characterizing changes in substrate supply and energy metabolism and their modulation by signaling pathways, and mitochondrial biogenesis in brain as a function of age as well as the potential role of lipoic acid in restoring normal brain energy metabolism via thiol-disulfide exchange reactions.

Results

Effects of lipoic acid on brain glucose uptake and glucose transporter expression

Fig. 1A shows the [^{18}F]-FDG-PET images (dynamic microPET scanning) of 6- and 24 month-old male rat brains. The standardized glucose uptake value (SUV) that assesses the kinetics of glucose uptake, in the 24 month-old rat brain was significantly lower (~14%) than that in the 6 month-old rat brain at the end of the scan (Fig. 1B). There were no

NIH-PA Author Manuscript

NIH-PA Author Manuscript

NIH-PA Author Manuscript

significant differences between 6- and 12 month-old SUV values. Lipoic acid (0.23% wt/vol in the drinking water for 3 weeks) increased SUV by ~40% in the 24 month-old rat brains (Fig. 1A,B) but had no effect at younger ages.

Expression of glucose transporters, which is closely related to glucose supply to the brain, is shown in Fig. 2. The protein level of neuronal glucose transporter 3 (GLUT3) decreased by 30% in 24 month-old rat brains compared to the 6 month-old brains, whereas lipoic acid treatment partly restored GLUT3 in the 24 month-old group (Fig. 2C). Likewise, neuronal GLUT4 expression decreased sharply with age, and lipoic acid treatment restored its expression slightly (Fig. 2D). GLUT1 (55 kDa), across the blood brain barrier, decreased marginally as a function of age; lipoic acid, however, had no effect on its expression (Fig. 2A). Interestingly, expression of the glial glucose transporter, GLUT1 (45 kDa) increased with age, and lipoic acid treatment had no effect on its expression (Fig. 2B). It is well established that insulin signaling promotes the translocation of GLUT4 from a mobilizable pool to the plasma membrane (Grillo *et al.* 2009). Fig. 2E shows that membrane-bound GLUT4 does not change significantly with age but lipoic acid facilitates increased expression of membrane-bound GLUT4 (ratio of GLUT4 in the plasma membrane fraction over that in total membrane fraction) in 6- and 24 month-old rat brains (Fig. 2E).

Effects of lipoic acid on Akt- and JNK signaling pathways

Phosphorylation of Akt on Ser^{473} by upstream signals results in its activation; phosphorylation on Thr^{308} is largely constitutive. Phosphorylation of Akt at Ser^{473} in brain cortices from 24 month-old rats is substantially lower than that from 6 month-old rats; treatment with lipoic acid significantly increased the levels of Akt phosphorylation (Fig. 3A). Phosphorylation of GSK3β at Ser^{9} by Akt results in its inhibition: the percentage of GSK3β phosphorylated at Ser^{9} decreases with age and lipoic acid significantly increased inhibition of GSK3β (and, thereby its pro-apoptotic effects) in 12- and 24 month-old rat brains (Fig. 3B). The effects of lipoic acid on Akt activation (Fig. 3A) tally with those on GSK3β inhibition (Fig. 3B).

JNK activation (phosphorylation) increases with age (Fig. 3C) and dissimilar effects of lipoic acid were observed on different age groups: lipoic acid increased pJNK expression levels in 6 month-old rat brains, whereas it decreased pJNK levels in 24 month-old rat brains (Fig. 3C). The overall effect of lipoic acid seems to maintain a similar relative activity of JNK to Akt pathways in brain cortices from 6- and 24 month-old rats: this notion is supported by the pJNK/pAkt ratios depicted in Fig. 3D.

Residing upstream in the insulin pathway, IRS1 bridges insulin receptor and PI3K and is essential for the activation of PI3K/Akt signaling cascade. Phosphorylation of IRS1 at Tyr^{608} is required for the interaction of IRS1 with PI3K and the subsequent activation of PI3K/Akt pathway (Sun *et al.* 1993; Rocchi *et al.* 1995). Conversely, phosphorylation of IRS1 at Ser^{307} is inhibitory and mediated by JNK, placing it as a pivotal node in the crosstalk between the JNK and PI3K/Akt pathways. The levels of IRS1 phosphorylated at Ser^{307} increase in rat brains as a function of age (Fig. 3E) whereas those phosphorylated at Tyr^{608} show a slight decrease (Fig. 3F). Lipoic acid increased Tyr^{608} phosphorylation and decreased Ser^{307} phosphorylation of IRS1; the effects were more pronounced in old animals (24 month-old rat brains) (Fig. 3E,F). The decrease in Ser^{307} phosphorylation of IRS1 elicited by lipoic acid matched its effect on the pJNK/pAkt ratios (Fig. 3D).

Insulin-like effect of lipoic acid on cellular bioenergetics

Supplementation of primary cortical neurons with lipoic acid resulted in a substantial increase of oxygen consumption rates (OCR) (Fig. 4A): lipoic acid increased basal

NIH-PA Author Manuscript

NIH-PA Author Manuscript

NIH-PA Author Manuscript

respiration, OXPHOS-induced respiration, and maximal respiratory capacity by 27.3-, 33.7-, and 37.5%, respectively. The reserve capacity was augmented by 47.6% by lipoic acid (Table 1). These enhancing effects by lipoic acid were suppressed by LY294002, a specific inhibitor of PI3K; this may be interpreted as lipoic acid exerting its effects upstream of PI3K and in agreement with the increased levels of IRS1 phosphorylated at Tyr^{608} (Fig. 3F). (Similar effects of lipoic acid were observed in a mixture of hippocampal/cortical neurons from a triplet transgenic mouse model of Alzheimer's disease). The lipoic acid-mediated increase in the bioenergetic parameters may be accounted for in terms of an increase in mitochondrial density in primary cortical neurons (pre-treated with 20 μM lipoic acid for 18 h) as shown by the increased expression of pyruvate dehydrogenase $E_{1\alpha}$ subunit (thus enhancing acetyl-CoA supply to the tricarboxylic acid cycle) and of α-ketoglutarate dehydrogenase (Fig. 4B) and by the DNA_{mit}/DNA_{nu} values (COX3 and 18SrDNA representing mitochondrial genome and nuclear genome, respectively) (Fig. 4D); the former data were confirmed by the increased protein expression of pyruvate dehydrogenase $E_{1\alpha}$ subunit, α-ketoglutarate dehydrogenase, and complexes II and V of the mitochondrial respiratory chain (Fig. 4C). The latter, COX3/18SrDNA ratios, indicate that the increase in mitochondrial density elicited by lipoic acid supplementation was inhibited by LY294002 and compound C, inhibitors of PI3K and AMPK, respectively (Fig. 4D). The role of AMPK in mitochondrial biogenesis is further examined in Fig. 5.

Lipoic acid activates AMPK-Sirt1-PGC1α-NRF1 transcriptional pathway and stimulates mitochondrial biogenesis

The full activation of PGC1α –the master regulator of mitochondrial biogenesis– requires its phosphorylation and deacetylation. The phosphorylation of PGC1α by AMPK at Thr^{177} and Ser^{538} appears to be a requirement for the induction of the PGC1α promoter (Jager *et al.* 2007). AMPK is activated through the phosphorylation at Thr^{172} on the α (catalytic) subunit; the levels of AMPK phosphorylated at Thr^{172} decreased with age whereas lipoic acid elicited a robust increase of active AMPK in the brain of 12- and 24-month-old rats (Fig. 5A). Also, PGC1α phosphorylation by AMPK facilitates the subsequent deacetylation by Sirt1 (Canto *et al.* 2009). The expression level of Sirt1, a NAD-dependent deacetylase, remained unchanged during aging but treatment with lipoic acid significantly increased Sirt1 expression in the brain of 24 month-old rats (Fig. 5B).

The total PGC1α expression in rat brain cortex decreased as a function of age and lipoic acid elicited a slight but significant enhancement of the expression levels in the brain cortex of 24 month-old rats (Fig. 5C). The activity of PGC1α is negatively correlated with its relative acetylation level, which was significantly decreased in the brain of 24 month-old rats upon lipoic acid treatment (Fig. 5D). It may be surmised that brain aging is associated with an apparent decrease in PGC1α expression and activity and that the effects of lipoic acid are more evident at old ages.

NRF1 has been identified as a downstream target of PGC1α and an important transcription factor for mitochondrial biogenesis that not only stimulates the expression of mitochondrial proteins such as OxPhos components but also regulates the expression of Tfam and thereby affects mtDNA replication and expression (Scarpulla 2008). The activation of NRF1 requires the interaction with PGC1α, and hence it is not surprising that its expression is regulated by AMPK (Bergeron *et al.* 2001). NRF1 expression levels decreased as a function of age (Fig. 5E), and lipoic acid increased its expression in the brains of both 6- and 24 month-old rats.

Taken together, a decreased AMPK-Sirt1-PGC1α-NRF1 transcriptional pathway as a function of age results in diminished mitochondrial biogenesis; accordingly, DNA_{mit}/DNA_{nu} values (COX3 and 18SrDNA representing mitochondrial genome and nuclear genome,

NIH-PA Author Manuscript

NIH-PA Author Manuscript

NIH-PA Author Manuscript

respectively) decreased with age (Fig. 5F). As before, lipoic acid treatment enhanced mitochondrial biogenesis in brain of old animals (Fig. 5F).

Lipoic acid rescues the decline in mitochondrial bioenergetics associated with age

Data shown on the effects of lipoic acid on the different components of the AMPK-Sirt1-PGC1α transcriptional pathway and resulting in enhanced mitochondrial biogenesis (Fig. 5) suggest a more robust mitochondrial bioenergetic efficiency. Accordingly, lipoic acid treatment augmented brain cortex ATP levels (Fig. 6A); ATP content in 24 month-old rats was only 70% of that in their younger counterparts, while lipoic acid treatment increased it by 15% (Fig. 6A). The increased ATP levels in the brain cortex of 24 month-old rats was associated with a substantial increase (41%) in ATP synthase activity (Fig. 6B). It was shown previously that the respiratory control ratios (RCR) of rat brain mitochondria respiring on complex I substrates (glutamate/malate) decreased as a function of age, and the decline is accounted for largely by an increase in state 4 respiration while state 3 respiration remained somehow constant (Lam *et al.* 2009). Consistent with this observation, lipoic acid increased the respiratory control ratio of brain cortical mitochondria, an effect mainly driven by a diminished state 4 respiration (20%); the latter effect correlated with decreased formation of H_2O_2 during state 4 respiration (Fig. 6C,D).

Pyruvate dehydrogenase (PDH) catalyzes the oxidative decarboxylation of pyruvate to acetyl-CoA, thus furnishing substrates for the tricarboxylic acid cycle. Inactivation of PDH occurs upon phosphorylation in the $E_{1\alpha}$ subunit; hence, an increase in pPDH/PDH values is associated with limited delivery of activated carbon units to the tricarboxylic acid cycle and diminished formation of reducing equivalents to support respiratory chain activity. Fig. 6E shows a substantial increase in the pPDH/PDH ratio in the brain of 24 month-old rats as compared with that of 6 month-old animals; these effects are ameliorated by treatment with lipoic acid. It is noteworthy, that JNK activation (bisphosphorylation) was reported to increase with age in rat brain as well as it translocation to mitochondria where it triggers a phosphorylation cascade that results in phosphorylation (inhibition) of the $E_{1\alpha}$ subunit of PDH (Zhou *et al.* 2008). The effect of lipoic acid on PDH activity is highly likely driven by its inhibition of JNK (see Fig. 3C).

The expression levels of Complex II-SDHB, COX-I, and CV-α of the mitochondrial respiratory chain decreased with age; in every instance, lipoic acid treatment resulted in an increased expression of the aforementioned complexes in the brains of 24 month-old rats (Fig. 6F). Lipoic acid significantly increased complex I activity (30%), whereas there was no significant effect on complex IV activity (not shown).

Discussion

This study characterized the age-associated impairment in brain glucose uptake, mitochondrial bioenergetics and biogenesis, and the regulatory signaling and transcriptional pathways that impinge on the mitochondrial energy-transducing capacity. The beneficial effects of lipoic acid on energy metabolism in brain cortex reported here are interpreted in terms of lipoic acid-mediated regulation of redox-sensitive regulatory pathways via thiol-disulfide exchange reactions. A direct interaction of lipoic acid with covalently bound lipoamide in the pyruvate dehydrogenase and α-ketoglutarate dehydrogenase complexes is ruled out because exogenously administered lipoic acid cannot equilibrate with these cofactors.

Insulin signaling affects various aspects of energy metabolism: active Akt promotes glucose uptake, translocates to mitochondria in human neuroblastoma cells (Bijur & Jope 2003), and is suggested to maintain mitochondrial electron-transport chain integrity by suppressing

NIH-PA Author Manuscript

NIH-PA Author Manuscript

NIH-PA Author Manuscript

FOXO1/HMOX1 and preventing heme depletion (Cheng *et al.* 2010). Insulin resistance is a pronounced pathological phenomenon in age-related diseases, as aging is associated with decreases in the levels of both insulin and its receptor (Frölich *et al.* 1998). Although chronic exposure to high level of oxidative stress could alter mitochondrial function and cause insulin resistance, modest oxidative conditions are actually required for the activation of insulin signaling (Cho *et al.* 2003). Therefore the effect of lipoic acid on insulin signaling most likely lies in its pro-oxidant feature, oxidizing critical cysteine residues to disulfides. Possible targets of lipoic acid-mediated oxidation could be the ones with abundant cysteine residues, including insulin receptors (Cho *et al.* 2003; Storozhevykh *et al.* 2007), IRS1, and phosphatases (PTEN and PTP1B) (Barrett *et al.* 1999; Loh *et al.* 2009). These thiol/disulfide exchange reactions are likely the basis for the effects of lipoic acid in increasing phospho-Tyr^{608} (Fig. 3F) and decreasing phospho-Ser^{307} (Fig. 3E) on IRS1. These effects are supported by the observation that the enhancing effect of lipoic acid on mitochondrial basal respiration and maximal respiratory capacity was sensitive to PI3K inhibition (Fig. 4A), thus suggesting that lipoic acid acted upstream of PI3K with IRS1 as one of the most plausible targets. As downstream targets of Akt signaling, the trafficking of GLUT4 to the plasma membrane was induced by lipoic acid treatment. The effect of lipoic acid on the biosynthesis of glucose transporters was also insulin-dependent, for chronic insulin administration induced biosynthetic elevation of GLUT3 in rat brain neurons and L6 muscle cells (Bilan *et al.* 1992; Taha *et al.* 1995; Uehara *et al.* 1997). Therefore increased efficiency of glucose uptake into brain by lipoic acid could at least partly be accounted for by its insulin-like effect.

JNK activation increases in rat brain as a function of age as well as JNK translocation to mitochondria and impairment of energy metabolism upon phosphorylation of the $E_{1\alpha}$ subunit of the pyruvate dehydrogenase complex (Zhou *et al.* 2009). Data in this study indicate that lipoic acid decreases JNK activation at old ages; this effect might be due to the attenuation of cellular oxidative stress responses; in this context, lipoic acid was shown to replenish the intracellular GSH pool (Busse *et al.* 1992; Suh *et al.* 2004).

Cross-talk between the PI3K/Akt route of insulin signaling and JNK signaling is expressed partly as the inhibitory phosphorylation at Ser^{307} on IRS1 by JNK, thus identifying the JNK pathway as a negative feedback of insulin signaling by counteracting the insulin-induced phosphorylation of IRS1 at Tyr^{608}. Likewise, FoxO is negatively regulated by the PI3K/Akt pathway and activated by the JNK pathway (Karpac & Jasper 2009). Overall, insulin signaling has a positive impact on energy metabolism and neuronal survival but its aberrant activation could lead to tumor and obesity (Finocchietto *et al.* 2011); JNK activation adversely affects mitochondrial energy-transducing capacity and induces neuronal death, but it is also required for brain development and memory formation (Mehan *et al.* 2011). A balance between these survival and death pathways determines neuronal function; as shown in Fig. 3D, lipoic acid restores this balance (pJNK/pAkt) that is disrupted in brain aging: in aged animals, lipoic acid sustained energy metabolism by activating the Akt pathway and suppressing the JNK pathway; in young animals, increased JNK activity by lipoic acid met up with the high insulin activity to overcome insulin over-activation and was required for the neuronal development.

Given the central role of mitochondria in energy metabolism, mitochondrial biogenesis is implicated in various diseases. Fewer mitochondria are found in skeletal muscle of insulin-resistant, obese, or diabetic subjects (Kelley *et al.* 2002; Morino *et al.* 2005). Similarly, $PGC1\alpha^{-/-}$ mice have reduced mitochondrial oxidative capacity in skeletal muscle (Lin *et al.* 2004). Data from this study showed a reduced mitochondrial density and decreased expression and activity of PGC1α in brain with age: evidence for the downregulation of the AMPK - Sirt1 pathway and the PGC1α downstream effector NRF1 is shown in Fig. 5.

NIH-PA Author Manuscript

NIH-PA Author Manuscript

NIH-PA Author Manuscript

Lipoic acid significantly enhanced mitochondrial biogenesis especially in old rats probably through the activation of AMPK-Sirt1-PGC1α-NRF1 (Fig. 5). Mitochondrial biogenesis appears to be regulated by both insulin- and AMPK signaling, as shown by changes in COX3/18SrDNA ratios by inhibitors of PI3K and AMPK (Fig. 4D).

The increase in bioenergetic efficiency (ATP production) by lipoic acid was associated with enhanced mitochondrial respiration and increased expression and catalytic activity of respiratory complexes (Fig. 6). However, this bioenergetic efficiency is dependent on concerted action by glucose uptake, glycolysis, cytosolic signaling and transcriptional pathways, and mitochondrial metabolism. The enhancement of mitochondrial bioenergetics by lipoic acid may be driven by its insulin-like effect (evidenced by the insulin-dependent increase in mitochondrial respiration in primary neurons) and by the activation of the PGC1α transcriptional pathway leading to increased biogenesis (evidenced by increasing expression of key bioenergetics components such as complex V, PDH, and α-KGDH upon lipoic acid treatment).

The observation that AMPK activity declines with age in brain cortex suggests an impaired responsiveness of AMPK pathway to the cellular energy status. The activation of AMPK requires Thr^{172} phosphorylation by LKB1 and CaMKKβ with a 100-fold increase in activity, followed by a 10-fold allosteric activation by AMP (Hardie *et al.* 2012). It is highly likely that loss of AMPK response to AMP allosteric activation is due to the impaired activity of upstream kinases. Lipoic acid may act as a mild and temporary stress that activates AMPK, the PGC1α transcriptional pathway, and mitochondrial biogenesis, thereby accounting for increases in basal and maximal respiratory capacity that enables vulnerable neurons in aged animals to adequately respond to energy deficit, achieving a long-term neuroprotective effect. Hence, activation of PGC1α by lipoic acid serves as a strategy to ameliorate brain energy deficits in aging. PGC1α transgenic mice demonstrated enhanced neuronal protection and altered progression of amyotrophic lateral sclerosis (Liang *et al.* 2011) and preserved mitochondrial function and muscle integrity during aging (Wenz *et al.* 2009).

Overall, data in this study unveil an altered metabolic triad in brain aging, entailing a regulatory devise encompassed by mitochondrial function (mitochondrial biogenesis and bioenergetics), signaling cascades, and transcriptional pathways, thus establishing a concerted mitochondria/cytosol/nucleus communication. Specifically, brain aging is associated with the aberrant signaling and transcriptional pathways that impinge on all aspects of energy metabolism including glucose supply and mitochondrial metabolism. Mitochondrial metabolism, in turn, modifies cellular redox- and energy- sensitive regulatory pathways; these constitute a vicious cycle leading to a hypometabolic state in aging. The prominent effect of lipoic acid in rescuing the metabolic triad in brain aging is accomplished through modulation of regulatory pathways, achieving an insulin-like effect: augmenting glucose uptake, restoring the Akt/JNK balance, enhancing mitochondrial bioenergetics, and supporting transcriptional pathways that foster mitochondrial biogenesis. Moreover, lipoic acid has been reported as potential therapeutic/nutritional agent in multiple age-related disease models: lipoic acid has been found to restore the age-dependent impairment of long-term potentiation (LTP) and glutamate release in rat hippocampus (McGahon *et al.* 1999); lipoic acid in combination with L-acetyl-carnitine restores mitochondrial biogenesis in the hippocampus (Aliev *et al.* 2009) and protected cortical neurons against β-amyloid and H_2O_2 toxic insults (Zhang *et al.* 2001).

NIH-PA Author Manuscript

NIH-PA Author Manuscript

NIH-PA Author Manuscript

Experimental Procedures

Animals and lipoic acid supplement

Male Fisher 344 rats of different ages (6, 12 and 24 months) were purchased from the National Institute of Ageing (NIA). Each rat was individually housed in the animal facility under standard conditions (12/12 light-dark cycle, humidity at 50 ± 15%, temperature 22 ± 2°C and 12 air changes/h). Rats at different ages (6-, 12- and 24 month old) were fed with 0.23% (wt/vol) R-(+)-lipoic acid in the drinking water for 3 weeks. Age-matched rats fed with normal water were used as control groups. All procedures were approved by the local Animal Care and Use Committee. The examined lipoic acid concentrations (0.08%, 0.14%, and 0.23% (wt/vol) estimated 40.5-, 60.3-, and 99.1 mg/kg per day) in drinking water for 3 weeks revealed that 0.23% (wt/vol) was more effective in most biochemical assays. Food intake was not affected by lipoic acid supplementation during the three weeks of treatment and there was no statistically significant difference in body weight between control group and lipoic acid–supplemented group.

Isolation of rat brain mitochondria

Upon completion of LA treatment, both LA-treated and control groups were sacrificed after euthanasia by CO_2 inhalation for 1–2 min and the brains were rapidly dissected on ice. Cerebellum, brain stem, and hippocampi were removed and the cortices were rapidly minced and homogenized at 4°C in mitochondrial isolation buffer (MIB) (pH 7.4), containing sucrose (250 mM), HEPES (20 mM), EDTA (1 mM), EGTA (1 mM), plus 0. 5% (w/v) bovine serum albumin and freshly supplemented with 25 μl/100 ml protease inhibitor cocktail, and 100 μl/100 ml phosphatase inhibitors. A portion of the cortex homogenates was collected for the Western Blot analysis and the rest were then centrifuged at 1500*g* for 5 min. The post-nuclear supernatants were collected and crude mitochondria were pelleted by centrifugation at 21,000*g* for 10 min. The resulting mitochondrial pellet was resuspended in 15% Percoll made in MIB, layered over a preformed 23%/40% Percoll discontinuous gradient, and centrifuged at 31,000*g* for 10 min. The purified mitochondria were collected at the 23%/40% interface and washed with 10 mL MIB by centrifugation at 16,700*g* for 15 min. The loose pellet was collected and transferred to a microcentrifuge tube and washed in MIB by centrifugation at 9000*g* for 8 min. The resulting mitochondrial pellet was resuspended in MIB to an approximate concentration of 5 mg/mL. Mitochondrial samples were used immediately for respiratory measurements or stored at −80°C for later protein and enzymatic assays. The purity of the mitochondrial fraction was assessed as previously described (Zhou *et al.* 2008).

Membrane preparation

Isolation of membrane-containing fractions was performed as described previously (Piroli *et al.* 2007; Grillo *et al.* 2009). Briefly, rats were decapitated and brain cortices were isolated, frozen on dry ice and stored at −70 °C until use. Brain cortices from each individual rat was homogenized in ice-cold homogenization buffer (0.32 M sucrose, 2 mM EDTA, 2 mM EGTA, 20 mM HEPES, with 25 μl/100 ml protease inhibitor cocktail, 100 μl/100 ml phosphatase inhibitors) and centrifuged for 10 min at 500 *g* at 4°C. The total membrane fraction (supernatant) was saved; a portion of this fraction was centrifuged at 31,000 *g* for 30 min at 4°C. The resulting pellet, which contained the plasma membrane fraction, was resuspended in PBS. Protein concentrations of the total membrane fraction and the plasma membrane fraction were determined by the method of Bradford (1976) using bovine serum albumin (BSA) as a standard.

NIH-PA Author Manuscript

NIH-PA Author Manuscript

NIH-PA Author Manuscript

DNA isolation and quantification

Total DNA from rat brain was prepared using Wizard Genomic DNA Purification Kit (Promega Corporation, Madison, WI, USA) and following the manufacturer's instructions. The relative copy numbers of mitochondrial and nuclear DNA were determined by real-time PCR with primers specific to the COX3 (mitochondrial) and 18SrDNA (nuclear) genes, 100 ng DNA, and SYBRGreen PCR master mix (Bio-Rad, Hercules, CA, USA) on an iCycler real-time PCR machine (Bio-Rad).

MicroPET imaging

MicroPET imaging was conducted at the Molecular Imaging Center at the Department of Radiology, University of Southern California, under the guidance of Dr. Peter Conti. Briefly, both LA treated and control groups were fasted for 6 h on a water only diet and then sedated using 2% isoflurane by inhalation and administered the radio tracer 2-deoxy-2 [^{18}F]fluoro-D-glucose intravenously. Blood for glucose concentration was measured before the administration of the tracer to ensure that changes in glucose metabolism during [^{18}F]-FDG-PET imaging were not due to differences in starting blood glucose levels but the intrinsic activity of the brain. Rats were placed on a scanner bed with a warming bed to maintain animal body temperature and underwent scanning for duration of 10 min using a Siemens MicroPET R4 scanner with a 19 cm (transaxial) by 7.6 cm (axial) field of view. This system has an absolute sensitivity of 4% with a spatial resolution of ~1.3 mm at the center of view. This is a non-invasive technique and the rats were sedated during the entire duration. Additionally, the rats underwent microCT scanning for 5 min (Siemens Inveon) with intravenous contrast material for coregistration with microPET (AMIDE, Free Software Foundation, Inc., Boston, MA, USA). This provides high resolution (~1 mm) information of brain structure and enables identification in the extent of brain atrophy. Region of Interest (ROI) was defined (AMIDE, Free Software Foundation, Inc., Boston, MA), and Standard Uptake Values (SUV) was calculated based also on dose, time, and body weight.

Polarographic assays and ATP measurements

Oxygen consumption was measured with a Clarktype electrode (Hansatech, Norfolk, UK) assembled to a thermostatic water jacket. The assay buffer consisted of 70 mM sucrose, 220 mM mannitol, 10 mM KH_2PO4, 5 mM $MgCl_2$, 1 mM EGTA, 2 mM HEPES, and 0.5% (w/v) bovine serum albumin, pH 7.4. The mitochondrial suspension was maintained under continuous stirring with a magnetic agitator in the electrode chamber. State 4 respiration was measured with complex I substrates (5 mM glutamate + 5 mM malate) and state 3 respiration in the presence of 0.41 mM ADP. Brain cortex homogenates were lysed in an equal volume of perchloric acid (2 M) and centrifuged for 10 min at 12000 *g*. Supernatants were neutralized with $KHCO_3$ (3 M) and recentrifuged at 12000 *g*. ATP in tissue extracts was quantitatively measured by a bioluminescence assay that uses recombinant firefly luciferase and D-luciferin (Invitrogen, Carlsbad, CA, USA).

Metabolic flux analysis

Primary cortical neurons from day 18 (E18) embryos of female Sprague-Dawley rats were cultured on Seahorse XF-24 (Seahorse BioSciences, Billerica, MA, USA) plates at a density of 75,000 cells/well. Neurons were grown in Neurobasal Medium + B27 supplement (Invitrogen, Carlsbad, CA, USA) for 10 days prior to experiment. Cells were treated with control vehicle, R-(+) lipoic acid (20 μM), LY294002 (50 μM), and R-(+) lipoic acid (20 μM) + LY294002 (50 μM), and the assays were conducted 18 h post-treatment. On the day of metabolic flux analysis, media was changed to unbuffered DMEM (DMEM base medium supplemented with 25-mM glucose, 1 mM sodium pyruvate, 31 mM NaCl, 2 mM GlutaMax (Invitrogen, Carlsbad, CA, USA); pH 7.4) and incubated at 37°C in a non-CO_2 incubator for

NIH-PA Author Manuscript

NIH-PA Author Manuscript

NIH-PA Author Manuscript

1 hour. All medium and injection reagents were adjusted to pH 7.4 on the day of assay. Using the Seahorse XF-24 (Seahorse BioSciences) metabolic analyzer, 3 baseline measurements of oxygen consumption rate (OCR) were sampled prior to sequential injection of mitochondrial inhibitors. Three metabolic determinations were sampled following addition of each mitochondrial inhibitor prior to injection of the subsequent inhibitors. The mitochondrial inhibitors used were oligomycin (4 μM), FCCP (carbonyl cyanide 4-(trifluoromethoxy)- phenylhydrazone) (1 μM), and rotenone (1 μM). OCR was automatically calculated and recorded by the Seahorse XF-24 software. After the assays, protein level was determined for each well to confirm equal cell density per well.

Enzyme activity assays and H_2O_2 measurement

ATPase (complex V) activity was measured in purified mitochondria from rat brain cortex: 10 μg of broken mitochondria were added to 200 μl reaction buffer containing 250 mM sucrose, 50 mM HEPES, pH 8.0, 5 mM $MgSO_4$, 2.5 mM sodium phosphoenolpyruvate, 2 μg antimycin, 1 μl of PK/LDH mixture, and 2.5 mM ATP. Reaction was initiated by addition of 0.35 mM NADH and initial rates were measured at 340 nm at 25°C (ε_{340} = 6.22 mM^{-1} cm^{-1}). Complex I activity was assessed in isolated mitochondria (20 μg) using Complex I Enzyme Activity Microplate Assay Kit (Mitosciences, Eugene, OR, USA) following the manufacturer's instructions. H_2O_2 generation from isolated brain cortical mitochondria was determined by the Amplex Red /Peroxidase Assay kit (Invitrogen, Carlsbad, CA, USA) following the manufacturer's instructions.

Immunoprecipitation

Immunoprecipitation was used to detect the lysine-acetylation levels of Sirtuin substrates, *i.e.*, PGC1α. Brain cortex homogenate was subjected to immunoprecipitation by using Pierce Coated Plate IP Kit. Immunoprecipitated proteins were boiled in non-reducing sample buffer (Thermo Scientific, Rockford, IL, USA) and then detected by Western blot.

Western blot analysis

Brain cortex homogenates and mitochondria were solubilized in SDS sample buffer, separated by SDS/PAGE, and transferred onto PVDF membranes. Using appropriate antibodies, the immunoreactive bands were visualized with an enhanced chemiluminescence reagent. The blots were quantified using UN-SCAN-IT gel 6.1 (Silk Scientific, Inc., Orem, UT, USA).

Immunocytochemistry

Primary cortical neurons from day 18 (E18) embryos of female Sprague-Dawley rats were cultured on pre-coated chamber slides. Neurons were grown in Neurobasal Medium +B27 supplement for 10 days prior to experiment. Cells were treated with either vehicle or R-(+)-lipoic acid (20 μM) for 18 h followed by fixation with 4% paraformaldehyde. For immuno-fluorescent staining, fixed cells were washed in PBS three times, and then blocked (1hr RT, PBS with 5% goat Serum and 0.5% triton x-100), immuno-stained using antibodies directed against PDH $E_{1\alpha}$ (1:200, 4°C overnight, Mitosciences, Eugene, OR, USA) and α-KGDH (1:200, 4°C overnight, Proteintech Group Inc, Chicago, IL, USA) followed by three times of washing and secondary antibodies Fluorescein goat anti-mouse and CY3-conjugated goat anti-rabbit (1:500, Chemicon, Ramona, CA, USA, 1h at RT) respectively. Slides were mounted with anti-fade mounting medium with DAPI (Vector Laboratories, Burlingame, CA, USA). Fluorescent images were taken using a fluorescent microscope, normalized and analyzed with the slide book software (Intelligent Imaging Innovations Inc, Santa Monica, CA, USA).

NIH-PA Author Manuscript

NIH-PA Author Manuscript

NIH-PA Author Manuscript

Statistical analysis

Number of animals for statistically significant outcomes in [^{18}F]-FDG-PET experiments was calculated as n = 5 to observe a significance of $P < 0.05$ for differences between control and treatment group averages with either 15% or 20% coefficient of variation (CV) (Eckelman et al., 2007). Data are reported as means ± SEM of at least 5–6 independent experiments. Significant differences between mean values were determined by Student t-test or one way analysis of variance (ANOVA) followed by a Newman-Keuls post hoc analysis.

Acknowledgments

Supported by NIH grant RO1AG016718 (to E.C.) and PO1AG026572 (to R.D.B.)

Abbreviations

LA	R-(+) lipoic acid
PGC1α	Peroxisome proliferator-activated receptor γ co-activator 1α
PDH	pyruvate dehydrogenase
JNK	c-Jun N-terminal kinases
NRF1	Nuclear respiratory factor 1
IRS1	Insulin Receptor Substrate 1
α-KGDH	α-ketoglutarate dehydrogenase
SDHB	succinate dehydrogenase iron-sulfur subunit
COX-I	Cytochrome c oxidase subunit one
CV-α/β	Complex V-α/β subunit

References

Aliev G, Liu J, Shenk JC, Fischbach K, Pacheco GJ, Chen SG, Obrenovich ME, Ward WF, Richardson AG, Smith MA, Gasimov E, Perry G, Ames BN. Neuronal mitochondrial amelioration by feeding acetyl-L-carnitine and lipoic acid to aged rats. J. Cell. Mol. Med. 2009; 13:320–333. [PubMed: 18373733]

Barrett WC, DeGnore JP, Keng YF, Zhang ZY, Yim MB, Chock PB. Roles of superoxide radical anion in signal transduction mediated by reversible regulation of protein-tyrosine phosphatase 1B. J. Biol. Chem. 1999; 274:34543–34546. [PubMed: 10574916]

Bergeron R, Ren JM, Cadman KS, Moore IK, Perret P, Pypaert M, Young LH, Semenkovich CF, Shulman GI. Chronic activation of AMP kinase results in NRF-1 activation and mitochondrial biogenesis. Am. J. Physiol. End. Metab. 2001; 281:E1340–D1346.

Bijur GN, Jope RS. Rapid accumulation of Akt in mitochondria following phosphatidylinositol 3-kinase activation. J. Neurochem. 2003; 87:1427–1435. [PubMed: 14713298]

Bilan PJ, Mitsumoto Y, Maher F, Simpson IA, Klip A. Detection of the GLUT3 facilitative glucose transporter in rat L6 muscle cells: regulation by cellular differentiation, insulin and insulin-like growth factor-I. Biochem. Biophys. Res. Comm. 1992; 186:1129–1137. [PubMed: 1497646]

Busse E, Zimmer G, Schopohl B, Kornhuber B. Influence of alpha-lipoic acid on intracellular glutathione in vitro and in vivo. Arzneimittelforschung. 1992; 42:829–831. [PubMed: 1418040]

Canto C, Gerhart-Hines Z, Feige JN, Lagouge M, Noriega L, Milne JC, Elliott PJ, Puigserver P, Auwerx J. AMPK regulates energy expenditure by modulating NAD^+ metabolism and SIRT1 activity. Nature. 2009; 458:1056–1060. [PubMed: 19262508]

Cheng Z, Tseng Y, White MF. Insulin signaling meets mitochondria in metabolism. Trends Endocrinol. Metab. 2010; 21:589–598. [PubMed: 20638297]

NIH-PA Author Manuscript

NIH-PA Author Manuscript

NIH-PA Author Manuscript

Cho KJ, Moini H, Shon HK, Chung AS, Packer L. Alpha-lipoic acid decreases thiol reactivity of the insulin receptor and protein tyrosine phosphatase 1B in 3T3-L1 adipocytes. Biochem. Pharmacol. 2003; 66:849–858. [PubMed: 12948866]

Cohen HY, Miller C, Bitterman KJ, Wall NR, Hekking B, Kessler B, Howitz KT, Gorospe M, de Cabo R, Sinclair DA. Calorie restriction promotes mammalian cell survival by inducing the SIRT1 deacetylase. Science. 2004; 305:390–392. [PubMed: 15205477]

Finocchietto PV, Barreyro F, Peralta JG, Alippe Y, Giovambattista A, Carreras MC, Poderoso JJ. Defective leptin-AMP-dependent kinase pathway induces nitric oxide release and contributes to mitochondrial dysfunction and obesity in ob/ob mice. Antioxid. Redox Signal. 2011; 15:2395–2406. [PubMed: 21529143]

Frölich L, Blum-Degen D, Bernstein HG, Engelsberger S, Humrich J, Laufer S, Muschner D, Thalheimer A, Turk A, Hoyer S, Zochling R, Boissl KW, Jellinger K, Riederer P. Brain insulin and insulin receptors in aging and sporadic Alzheimer's disease. J. Neural. Transm. 1998; 105:423–438. [PubMed: 9720972]

Gibson GE, Blass JP, Beal MF, Bunik V. The a-ketoglutarate dehydrogenase complex: a mediator between mitochondria and oxidative stress in neurodegeneration. Mol. Neurobiol. 2004; 31:43–63. [PubMed: 15953811]

Grillo CA, Piroli GG, Hendry RM, Reagan LP. Insulin-stimulated translocation of GLUT4 to the plasma membrane in rat hippocampus is PI3-kinase dependent. Brain Res. 2009; 1296:35–45. [PubMed: 19679110]

Hardie DG, Ross FA, Hawley SA. AMPK: a nutrient and energy sensor that maintains energy homeostasis. Nature Mol. Cell Biol. 2012; 13:251–262.

Jager S, Handschin C, St-Pierre J, Spiegelman BM. AMP-activated protein kinase (AMPK) action in skeletal muscle via direct phosphorylation of PGC-1alpha. Proc. Natl. Acad. Sci. USA. 2007; 104:12017–12022. [PubMed: 17609368]

Karpac J, Jasper H. Insulin and JNK: optimizing metabollic homeostasis and lifespan. Trends Endocrinol. Metab. 2009; 20:100–106. [PubMed: 19251431]

Kelley DE, He J, Menshikova EV, Ritov VB. Dysfunction of mitochondria in human skeletal muscle in type 2 diabetes. Diabetes. 2002; 51:2944–2950. [PubMed: 12351431]

Lam PY, Yin F, Hamilton RT, Boveris A, Cadenas E. Elevated neuronal nitric oxide synthase expression during ageing and mitochondrial energy production. Free Radic. Res. 2009; 43:431–439. [PubMed: 19347761]

Liang H, Ward WF, Jang YC, Bhattacharya A, Bokov AF, Li Y, Jernigan A, Richardson A, Van Remmen H. PGC-1alpha protects neurons and alters disease progression in an amyotrophic lateral sclerosis mouse model. Muscle Nerve. 2011; 44:947–956. [PubMed: 22102466]

Lin J, Wu PH, Tarr PT, Lindenberg KS, St-Pierre J, Zhang CY, Mootha VK, Jager S, Vianna CR, Reznick RM, Cui L, Manieri M, Donovan MX, Wu Z, Cooper MP, Fan MC, Rohas LM, Zavacki AM, Cinti S, Shulman GI, Lowell BB, Krainc D, Spiegelman BM. Defects in adaptive energy metabolism with CNS-linked hyperactivity in PGC-1alpha null mice. Cell. 2004; 119:121–135. [PubMed: 15454086]

Loh K, Deng H, Fukushima A, Cai X, Boivin B, Galic S, Bruce C, Shields BJ, Skiba B, Ooms LM, Stepto N, Wu B, Mitchell CA, Tonks NK, Watt MJ, Febbraio MA, Crack PJ, Andrikopoulos S, Tiganis T. Reactive oxygen species enhance insulin sensitivity. Cell Metab. 2009; 10:260–272. [PubMed: 19808019]

McGahon BM, Martin DS, Horrobin DF, Lynch MA. Age-related changes in LTP and antioxidant defenses are reversed by an alpha-lipoic acid-enriched diet. Neurobiol. Aging. 1999; 20:655–664. [PubMed: 10674431]

Mehan S, Meena H, Sharma D, Sankhla R. JNK: a stress-activated protein kinase therapeutic strategies and involvement in Alzheimer's and various neurodegenerative abnormalities. J. Mol. Neurosci. 2011; 43:376–390. [PubMed: 20878262]

Morino K, Petersen KF, Dufour S, Befroy D, Frattini J, Shatzkes N, Neschen S, White MF, Bilz S, Sono S, Pypaert M, Shulman GI. Reduced mitochondrial density and increased IRS-1 serine phosphorylation in muscle of insulin-resistant offspring of type 2 diabetic parents. J. Clin. Invest. 2005; 115:3587–3593. [PubMed: 16284649]

NIH-PA Author Manuscript

NIH-PA Author Manuscript

NIH-PA Author Manuscript

Navarro A, Boveris A. The mitochondrial energy transduction system and the aging process. Am. J. Physiol. Cell Physiol. 2007; 292:C670–C686. [PubMed: 17020935]

Nemoto S, Takeda K, Yu ZX, Ferrans VJ, Finkel T. Role for mitochondrial oxidants as regulators of cellular metabolism. Mol. Cell Biol. 2000; 20:7311–7318. [PubMed: 10982848]

Onyango IG, Lu J, Rodova M, Lezi E, Crafter AB, Swerdlow RH. Regulation of neuron mitochondrial biogenesis and relevance to brain health. Biochim. Biophys. Acta. 2010; 1802:228–234. [PubMed: 19682571]

Patel, MS.; Packer, L., editors. Lipoid Acid. Energy production, antioxidant activity, and health effects. CRC Press, Taylor & Francis Group; Boca Raton: 2008.

Piroli GG, Grillo CA, Reznikov LR, Adams S, McEwen BS, Charron MJ, Reagan LP. Corticosterone impairs insulin-stimulated translocation of GLUT4 in the rat hippocampus. Neuroendocrinology. 2007; 85:71–80. [PubMed: 17426391]

Rocchi S, Tartare-Deckert S, Mothe I, Van Obberghen E. Identification by mutation of the tyrosine residues in the insulin receptor substrate-1 affecting association with the tyrosine phosphatase 2C and phosphatidylinositol 3-kinase. Endocrinology. 1995; 136:5291–5297. [PubMed: 7588273]

Scarpulla RC. Transcriptional paradigms in mammalian mitochondrial biogenesis and function. Physiol. Rev. 2008; 88:611–638. [PubMed: 18391175]

Shay KP, Moreau RF, Smith EJ, Smith AR, Hagen TM. Alpha-lipoic acid as a dietary supplement: molecular mechanisms and therapeutic potential. Biochim. Biophys. Acta. 2009; 1790:1149–1160. [PubMed: 19664690]

Storozhevykh TP, Senilova YE, Persiyantseva NA, Pinelis VG, Pomytkin IA. Mitochondrial respiratory chain is involved in insulin-stimulated hydrogen peroxide production and plays an integral role in insulin receptor autophosphorylation in neurons. BMC Neurosci. 2007; 8:84–91. [PubMed: 17919343]

Suh JH, Wang H, Liu RM, Liu J, Hagen TM. (R)-alpha-lipoic acid reverses the age-related loss in GSH redox status in post-mitotic tissues: evidence for increased cysteine requirement for GSH synthesis. Arch. Biochem. Biophys. 2004; 423:126–135. [PubMed: 14871476]

Sun XJ, Crimmins DL, Myers MG Jr. Miralpeix M, White MF. Pleiotropic insulin signals are engaged by multisite phosphorylation of IRS-1. Mol. Cell Biol. 1993; 13:7418–7428. [PubMed: 7504175]

Taha C, Mitsumoto Y, Liu Z, Skolnik EY, Klip A. The insulin-dependent biosynthesis of GLUT1 and GLUT3 glucose transporters in L6 muscle cells is mediated by distinct pathways. Roles of p21ras and pp70 S6 kinase. J. Biol. Chem. 1995; 270:24678–24681. [PubMed: 7559581]

Uehara Y, Nipper V, McCall AL. Chronic insulin hypoglycemia induces GLUT-3 protein in rat brain neurons. Am. J. Physiol. Endocrin. Metab. 1997; 272:E716–E719.

Wenz T, Rossi SG, Rotundo RL, Spiegelman BM, Moraes CT. Increased muscle PGC-1alpha expression protects from sarcopenia and metabolic disease during aging. Proc. Natl. Acad. Sci. USA. 2009; 106:20405–20410. [PubMed: 19918075]

Yin F, Boveris A, Cadenas E. Mitochondrial energy metabolism and redox signaling in brain aging and neurodegeneration. Antioxid. Redox Signal. 2012 in press.

Yin F, Jiang T, Cadenas E. Metabolic triad in brain aging: mitochondria, insulin/IGF-1 signalling, and JNK signalling. Biochem. Soc. Trans. 2013; 41:101–105. [PubMed: 23356266]

Zhang L, Xing GQ, Barker JL, Chang Y, Maric D, Ma W, Li BS, Rubinow DR. Alpha-lipoic acid protects rat cortical neurons against cell death induced by amyloid and hydrogen peroxide through the Akt signalling pathway. Neurosci. Lett. 2001; 312:125–128. [PubMed: 11602326]

Zhou Q, Lam PY, Han D, Cadenas E. c-Jun N-terminal kinase regulates mitochondrial bioenergetics by modulating pyruvate dehydrogenase activity in primary cortical neurons. J. Neurochem. 2008; 104:325–335. [PubMed: 17949412]

Zhou Q, Lam PY, Han D, Cadenas E. Activation of c-Jun-N-terminal kinase and decline of mitochondrial pyruvate dehydrogenase activity during brain aging. FEBS Lett. 2009; 583:1132–1140. [PubMed: 19272379]

NIH-PA Author Manuscript

NIH-PA Author Manuscript

NIH-PA Author Manuscript

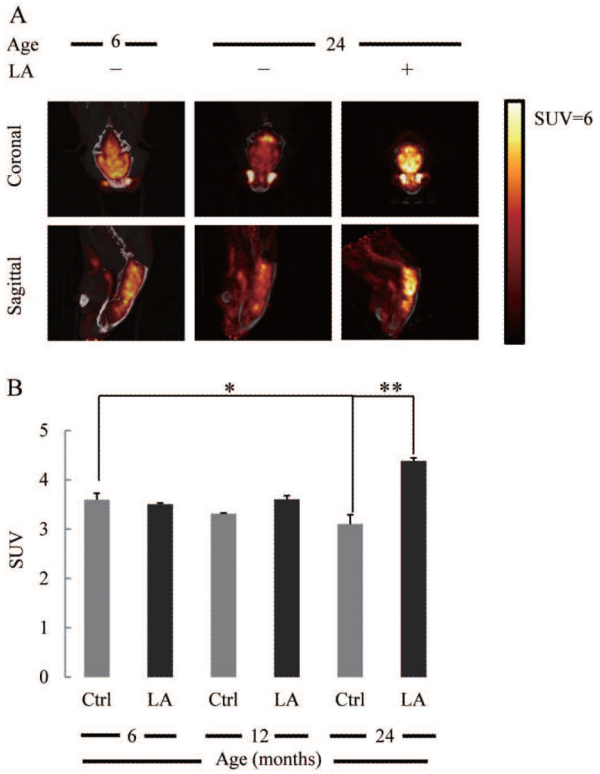

Fig. 1. Effect of lipoic acid on brain glucose uptake

(A) [^{18}F]-FDG microPET representative images of glucose uptake in 6-month control rats, 24-month control rats, and 24-month rats fed with lipoic acid as described in the Methods section. (B) Glucose Standard Uptake Values (SUV) as a function of age and effect of lipoic acid. *$p < 0.05$, $n = 6$.

NIH-PA Author Manuscript
NIH-PA Author Manuscript
NIH-PA Author Manuscript

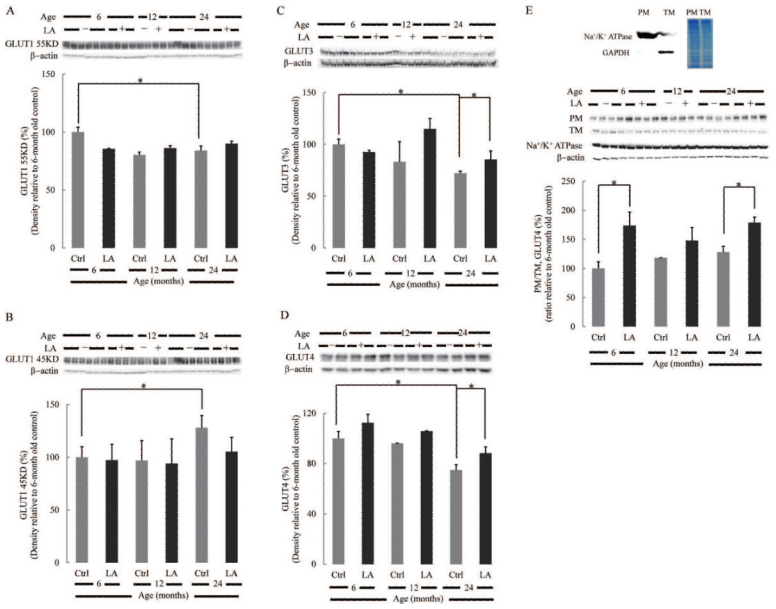

Fig. 2. Effect of lipoic acid on age-dependent changes in brain glucose transporters expression

Equal amount of homogenate samples from brain cortices of Fischer 344 rats were loaded on the gel. Expression of (A) endothelial GLUT1 55 kDa; (B) glial GLUT1 45 kDa; (C) neuronal GLUT3; (D) neuronal GLUT4. (E) Lipoic acid induced the translocation of GLUT4 from the cytosol to plasma membrane. GLUT4 translocation was assessed by the relative expression of GLUT4 on the plasma membrane fraction and total membrane. Na^+/K^+ ATPase and β-actin were used as loading control for plasma membrane and total membrane, respectively. Top panel: the purity of plasma membrane fraction was determined by Na^+/K^+ ATPase and GAPDH. *$p < 0.05$, $n \geq 6$.

NIH-PA Author Manuscript
NIH-PA Author Manuscript
NIH-PA Author Manuscript

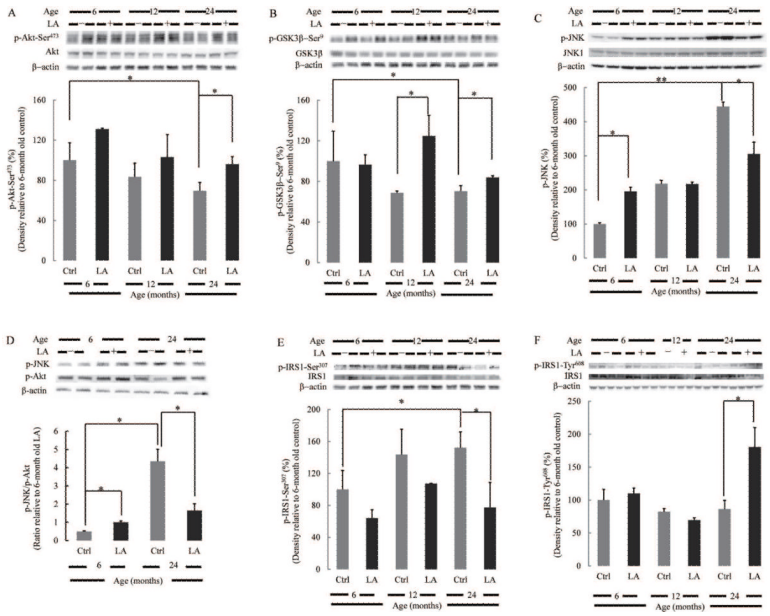

Fig. 3. Lipoic acid restored the age-induced imbalance of Akt/JNK signaling

Equal amount of homogenate samples from brain cortices of Fischer 344 rats were loaded on the gel. (A) Decreased activation (phosphorylation at Ser^{473}) of Akt with age. (B) Decreased inactivation (phosphorylation at Ser^{9}) of GSK3β with age. (C) Increased activation of JNK with age; lipoic acid increased JNK phosphorylation in the brain cortex homogenate from 6 month-old rats but decreased its phosphorylation in the brain cortex homogenate from 24 month-old rats. (D) Lipoic acid restored the age-associated imbalance of Akt/JNK signaling. Relative activity of JNK and Akt signaling was determined by assessing the relative active JNK and Akt levels on the same membrane. (E) Increased IRS1 Ser^{307} phosphorylation with age and reduction by lipoic acid. (F) Decreased IRS1 Tyr^{608} phosphorylation with age and restoration by lipoic acid.*$p < 0.05$, **$p < 0.01$, $n \geq 6$.

NIH-PA Author Manuscript

NIH-PA Author Manuscript

NIH-PA Author Manuscript

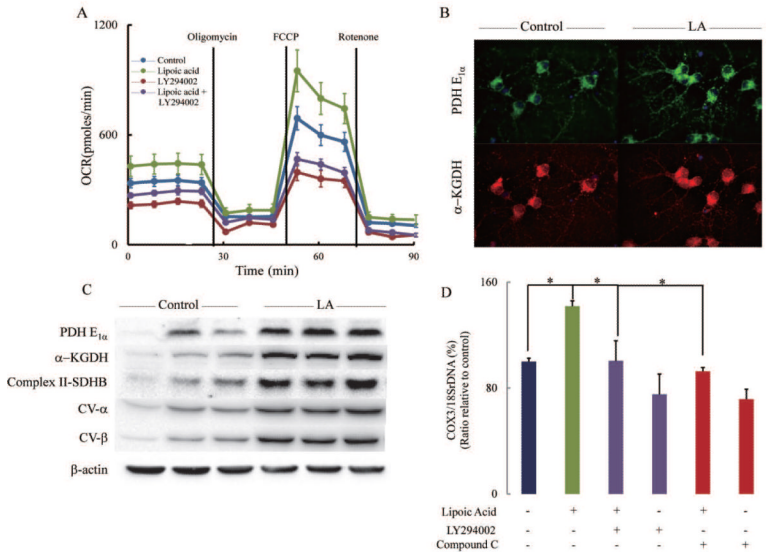

Fig. 4. Bioenergetics of primary cortical neurons

(A) Cells were treated with control vehicle, R-(+)-lipoic acid (20 μM), LY294002 (50 μM), and R-(+) lipoic acid (20 μM) + LY294002 (50 μM) for 18 h. Oxygen consumption rate (OCR) was determined using Seahorse XF-24 as described in the Methods section. (B) Lipoic acid increased expression of PDH-$E_{1\alpha}$ and α-KGDH. Cells were treated with vehicle or R-(+)-lipoic acid (20 μM) for 18 h before they were subjected to immuno-fluorescent staining. (C) Lipoic acid increased expression of Complex II-SDHB, CV-α, CV-β, PDH-$E_{1\alpha}$ and α-KGDH. After treated with vehicle or R-(+)-lipoic acid (20 μM) for 18 h, cells were harvested and lysed in Mammalian Protein Extraction Reagent (M-PER). (D) Lipoic acid increased mitochondrial density and was sensitive to PI3K (LY294002) and AMPK (compound C) inhibitors. $*p < 0.05$, $n = 5$ wells per group.

NIH-PA Author Manuscript

NIH-PA Author Manuscript

NIH-PA Author Manuscript

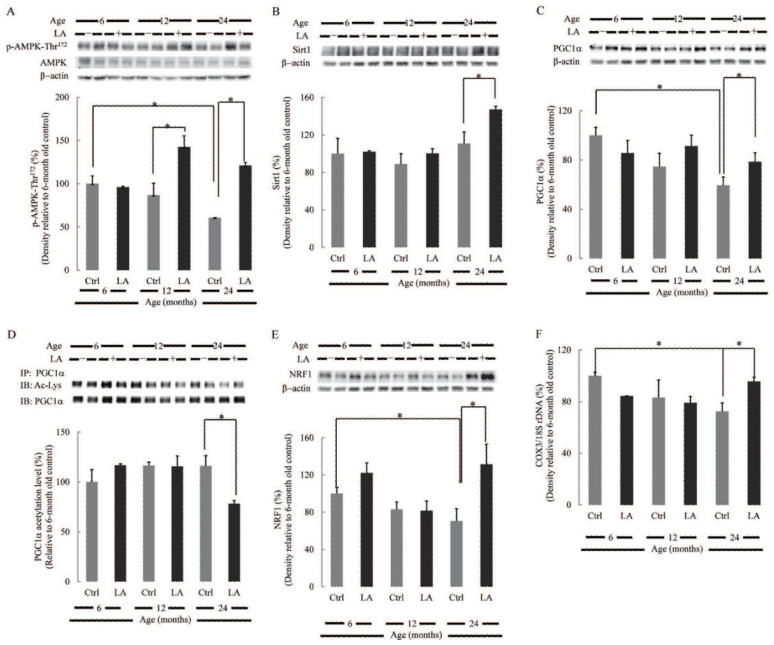

Fig. 5. Effect of lipoic acid on PGC1α transcriptional pathway and mitochondrial biogenesis

Equal amount of homogenate samples from brain cortices of Fischer 344 rats were loaded on the gel. Percentages (relative to 6-month old rats) of (A) p-AMPK-Thr^{172}; (B) Sirt1; (C) PGC1α; (D) PGC1α acetylation levels; (E) NRF1. (F) Mitochondrial biogenesis was assessed by the ratio of COX3/18SrDNA, determined by real-time PCR. *$p < 0.05$, $n \geq 6$.

NIH-PA Author Manuscript
NIH-PA Author Manuscript
NIH-PA Author Manuscript

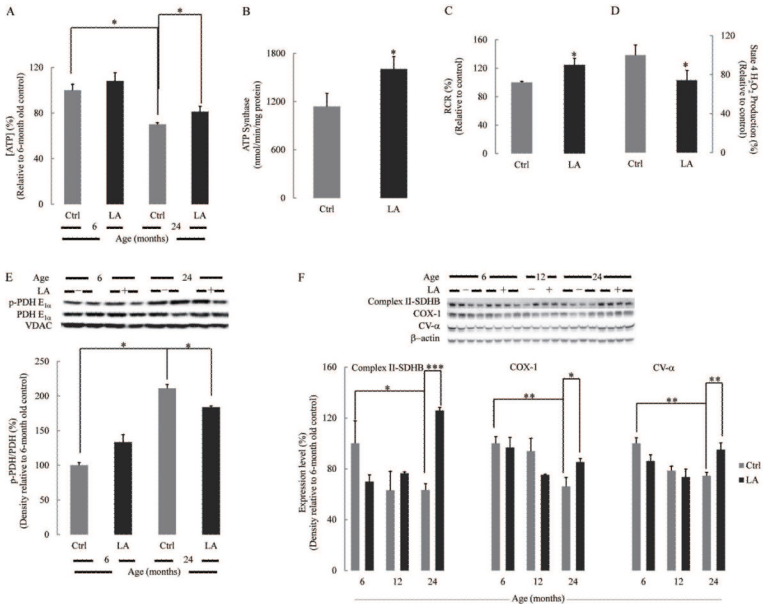

Fig. 6. Lipoic acid restored age-associated decline in mitochondrial bioenergetics in rat brain cortex

(A) ATP levels in the brain cortex homogenate of 6- and 24 month-old rats. (B) Effect of lipoic acid on ATPase activity of brain cortex mitochondria of 24 month-old rats. (C) Effect of lipoic acid on respiratory control ratios and (D) H_2O_2 production of brain cortex mitochondria of 24 month-old rats. (E) pPDH/PDH values in brain cortex mitochondria from 6- and 24 month-old rats. (F) Expression of complex II-SDHB, COX-1, and CV-α as a function of age. $*p < 0.05$, $**p < 0.01$, $***p < 0.001$, $n \geq 6$.

NIH-PA Author Manuscript

NIH-PA Author Manuscript

NIH-PA Author Manuscript

Table 1

Bioenergetic Parameters of Primary Cortical Neurons Effect of Lipoic Acid

	OCR (pmoles/min)			
	Control	**LA**	**LY294002**	**LA + LY294002**
Basal respiration	344 ± 27	439 ± 55 *	225 ± 18	285 ± 17 ψ
OXPHOS-induced respiration	190 ± 29	254 ± 63 *	124 ± 20	149 ± 21 ψ
H+ leak-induced respiration	154 ± 11	184 ± 31 *	100 ± 8	136 ± 12 ψ
Maximal respiratory capacity	691 ± 63	950 ± 114 *	396 ± 45	467 ± 36 ψ
Non-mitochondrial respiration	114 ± 10	142 ± 27 *	55 ± 7	66 ± 12 ψ
Reserve capacity	347 ± 69	512 ± 127 *	171 ± 49	182 ± 40 ψ

Assay conditions as described in the Methods section.

* $p < 0.05$ *versus* control.

ψ $p > 0.05$ *versus* lipoid acid treatment group.